High-speed automatic segmentation of intravascular stent struts in optical coherence tomography images

M. Han[a], D. Kim [a], W.Y. Oh [b], S. Ryu *[a]

[a]Dept. of Computer Science, KAIST, 291 Daehak-ro, Yuseong-gu, Daejeon 305-701, Republic of Korea; [b]Dept. of Mechanical Engineering, KAIST, 291 Daehak-ro, Yuseong-gu, Daejeon 305-701, Republic of Korea

ABSTRACT

Recently, Optical Coherence Tomography (OCT) has become one of the preferred clinical techniques for intracoronary diagnostic imaging. Thanks to its high resolution imaging capability, the OCT technique allows to identify microscopic features associated with various types of coronary plaque and to track of stent position, malaposition and neo-intimal tissue growth after stent implantation. Accurate visualization of stent struts can help to examine the status of implanted stents potentially leading to proper treatment of the coronary artery disease. However, unfortunately, current stent identification involves time-consuming segmentation algorithms sometimes requiring labor-intensive manual analysis process. To resolve the problem, we propose a high-speed automatic segmentation algorithm of intravascular stent struts in OCT images.

Unlike the other "automatic" stent segmentation algorithms, which are mainly based on time-consuming machine learning algorithms with manual addition and removal of stent struts for correction during the analysis process, our algorithm does not require any manual adjustments of stent struts. Our algorithm first analyzes 10 consecutive cross-sectional OCT images to take boundary information into account to enhance the accuracy of guide-wire segmentation and lumen segmentation. Then, it performs stent segmentation by automatically eliminating guide-wire signals using the previous segmentation results. The implementation of our algorithm uses the Intel(R) IPP library on CPU and the CUDA technology on GPU, which achieves the average analysis time of 0.28 s/frame and the detection rate ranging from 84% to 88.6% for about 120 continuous images per patient. As such, the proposed algorithm is robust and fast enough to be integrated in clinical routine.

Keywords: OCT images, stent segmentation, automatic segmentation, CUDA, GPU

1. INTRODUCTION

Heart disease has been one of the main causes of death, and the death probability of heart disease keeps growing over the recent years. Among various reasons for heart disease, coronary arteriosclerosis is dominant, thus coronary stent implantation is widely-used. Expanding the narrowed coronary arteries with stents to restore coronary artery blood flow has shown to be very effective, but like all invasive medical treatments, the stent placement procedure has some risks such as blood clotting within the vessel due to stent malapposition. In order to check that the procedure placed stents successfully, doctors check the stents right after the procedure in operating rooms, and they also check whether the stents are appropriately covered 6 or 12 months after the procedure.

The high resolution imaging capability of Optical Coherence Tomography (OCT) [1-3] enables accurate visualization of intravascular stent struts. Because the ultra high speed of the OCT system allows imaging of the 3-dimensional microstructure, it provides more detailed information about the stent struts to medical doctors so that they can treat the coronary artery disease more appropriately. Recent developments applied the OCT technology to identify pathologies in cardiovascular, retinal, and gastrointestinal tissues [4-6].

*sryu.cs@kaist.ac.kr; phone 82 42 350-3538; fax 82 42 350-3510

However, unfortunately, most of the current stent segmentation algorithms are based on time-consuming methods, such as machine learning. Therefore, they take much time [7-9], and some of them require manual adjustments of stent struts [9]. Such time-intensive algorithms may be useful for processing huge OCT image data outside operating rooms after the procedure, but they take too much time to be usable in operating rooms for clinicians to decide whether additional balloon inflation is needed. In this paper, we propose a high-speed automatic stent segmentation algorithm fast enough to be usable in operating rooms.

2. METHOD

The main contribution of our method is to develop a high-speed automatic stent segmentation algorithm usable in operating rooms when clinicians perform the stent placement procedure. Our segmentation algorithm is mostly automatic; after we set up some system-dependent parameters manually, the algorithm systematically processes the patient data without any intervention. Once we set up the parameters, we do not need to adjust them as long as the OCT system remains the same.

The overall structure of the algorithm is shown in Figure 1.

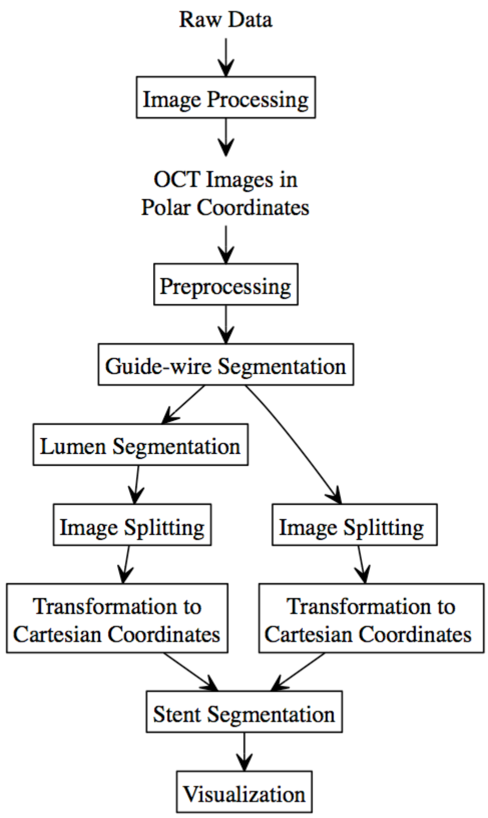

Figure 1. Flowchart of the algorithm

The algorithm takes raw binary data as its input and it visualizes the segmented stent information as its output. Instead of a complex, time-consuming, monolithic machine learning algorithm, our algorithm consists of a series of simple and fast algorithms. We describe each constituent algorithm in the following subsections.

2.1 Image processing

The algorithm begins with huge raw binary patient data. Because of the ultrahigh speed, high-resolution capability of the OCT system, the data for one patient is about 7 GB. To effectively process such a huge data, our algorithm uses the Intel® IPP library on CPU and the CUDA technology on GPU. The image processing algorithm itself consists of a series of small computations. The algorithm takes raw data and background data as inputs, where the background data is a constant data for a given OCT system. The algorithm processes the raw binary data in the granularity of A-lines. It first subtracts the background information from the raw data to achieve the actual patient data, and it adjusts the data by applying window functions such as Hanning and Gaussian window functions. It performs Fast Fourier Transformation (FFT) to binary data to get the signals in the electrical frequency domain, and it applies zero padding to align the data. It applies inverse-FFT to perform interpolation of the signals in the time domain, applies one more FFT on the interpolated and dispersion compensated signals, and finally achieves the resulting image by computing logarithmic scale intensity of the frequency signals. The algorithm results are OCT images in polar coordinates.

As the algorithm describes, all the computations of the image processing algorithm manipulates each A-line without using the information of other A-lines, which leads to the parallelization opportunity. Our image processing algorithm takes advantage of the embarrassingly parallel features of the CUDA technology on GPU, which improved the algorithm performance compared to its predecessor in MATLAB.

2.2 Preprocessing

Before performing any segmentation algorithms, we perform simple preprocessing steps to adjust the image data. We first remove trivial noises caused by a catheter and an optical fiber in each OCT image. To enhance the segmentation precision in the later steps, we blur each OCT image by applying the Average filter. Also, in order to enhance the accuracy of both guide-wire segmentation and lumen segmentation algorithms, we build "long images" by attaching 10 OCT images side by side. Even though each step of the algorithm uses one A-line at a time rather than using the information of arbitrary A-lines, the segmentation algorithms use local information such as nearby A-line information. By attaching 10 images, the algorithm can get nearby A-line information even for the edges of each image, which improves the precision of the segmentation algorithms.

2.3 Guide-wire segmentation

While most stent segmentation algorithms do not consider OCT images with guide wire or they remove guide wire during a preprocessing step, we segment guide-wire information and use it for stent segmentation. Unlike the existing approaches where treat guide-wire as a noise, we use the guide-wire information to improve the performance of later steps of the algorithm.

While a simple guide-wire segmentation algorithm would include many false alarms, we use the following three observations to reduce false positives. First, the position of a guide wire in each OCT image is always in the upper third of the image. Secondly, the position of a guide wire seldom changes between adjacent images. Finally, the size of a guide wire almost never changes between adjacent images.

Using these observations, we apply Otsu's threshold [10] to the long images we built in the preprocessing step to segment guide wire. We set up Region of Interest (ROI) and remove noises, which are not a guide-wire, by using the size of the guide-wire. Because the position of a guide wire in each image remains almost the same across different images, we identify the position pattern of the guide wire and segment guide wire in each image by using the pattern.

2.4 Lumen segmentation

In addition to the guide-wire segmentation, our algorithm performs lumen segmentation as well to improve the precision of the main stent segmentation. Our lumen segmentation is based on Z. Wang *et al.*'s algorithm [11]. The algorithm applies Otsu's threshold to OCT images and find the brightest pixel for each A-line as a lumen information for the A-line. When a detected lumen candidate is disconnected, the algorithm connects the disconnected pixels using interpolation.

However, their algorithm does not work well when it fails to find lumen information for either edge of an OCT image because it cannot apply interpolation on it. To resolve the problem, our algorithm uses the long images constructed by the preprocessing step to compensate the missing edge information. Using the adjacent images to get the edge information leads to more precise lumen segmentation as we verified with our experiments as described in the next Section. The algorithm also uses the size and the segmented information of guide wire, which removes more noises in this step.

2.5 Image splitting and transformation to Cartesian coordinates

The long images built at the preprocessing step improves the precisions of the guide-wire and lumen segmentation algorithms, but the adjacent image information for image edges is not helpful for our stent segmentation algorithm. Before performing the stent segmentation algorithm, we split the long images to single images by splitting one long image to 10 images with the original size. Also, we transform the images in Polar coordinates as produced by the image processing step to Cartesian coordinates, which are more appropriate for our stent segmentation algorithm as described below.

2.6 Stent segmentation

Like most automatic stent segmentation algorithms [12-15], our algorithm uses the properties of stents presented at each A-line. Such stent properties include the peak intensity and the existence of a shadow for each A-line. After selecting the stent candidates by using the properties, we use the results from both the guide-wire segmentation and the lumen segmentation algorithms to eliminate false positives. First, we eliminate the stent candidates which are actually guide wire by using the guide-wire segmentation results. Then, we eliminate false positives by calculating the average distance between the segmented lumen and the segmented stents and removing outliers. We use the images in Cartesian coordinates rather than in Polar coordinates, to process and visualize the coronary artery information without much distortion but more like the actual blood vessel. Thanks to pre-calculated segmentation information, the algorithm can reduce false positives and improve the accuracy of stent segmentation as we discuss in the next section.

2.7 Visualization

As we discussed so far, our stent segmentation is fully automatic after the initial set up of the parameters, thus it does not require any intervention or inputs from humans. After segmenting the stent information, the algorithm visualizes the segmented results so that medical doctors can verify the outcomes. The algorithm provides two kinds of result visualization: display of the segmented lumen and stents on images in Cartesian coordinates, and image of *en face* projection.

By providing the image in Cartesian coordinates rather than in Polar coordinates, the images look more close to the actual blood vessel, which make the medical doctor's job much easier. The medical doctors can easily identify the lumen and the stents from the image, and they can quickly detect stent malapposition from the segmented information. While each image shows a cross-sectional image of a vessel, the *en face* project image presents more information with longitudinal view of the vessel.

Currently, the visualization part is still under active development. We currently color the segmented lumen and stents by pixels, and we are working on clustering such nearby pixels. We are working on identifying stent malapposition automatically by using the distance between the lumen and stents, and we are also working on improving the visual quality of the *en face* project image.

3. RESULTS AND DISCUSSION

We experimented with our automatic stent segmentation algorithm with 3 sets of patient data, and the results of the experiments are shown in Table 1.

Table 1 The results of the automatic stent segmentation algorithm

Dataset Number	Number of Images	Number of Stents	Number of Segmented Stents	Accuracy (%)	Execution Time (sec)	Execution Time per Image (sec)
1	126	1,519	1,313	86.4	35.140	0.279
2	126	1,087	913	84	35.266	0.280
3	117	1,106	980	88.6	32.680	0.279
Total	369	3,712	3,206	86.4	103.086	0.279

The total number of images used is 369 and the total number of stents in the images is 3,712. Our algorithm segmented 3,206 stents, which amounts to the average accuracy of 86.4%. While the existing stent segmentation algorithms either do not report the execution time, or report 4 to 20 seconds per image, our algorithm takes 0.279 seconds per image which is unprecedented.

There is a clear trade-off between the speed and the accuracy of stent segmentation algorithms. To increase the accuracy, we should use complex computations such as machine learning, classification, and active contour methods, but they are often too expensive to be usable in operating rooms. On the contrary, to increase the execution performance, we should use simple but fast computations as we propose in this paper, but such methods may include too many false positives. We believe that our algorithm is fast enough to be usable in operating rooms right after the stent placement procedure so that the clinicians can decide whether an additional treatment is necessary or not. Also, our experimental results show that the accuracy of the high-speed algorithm is reasonable enough to be helpful for the clinicians to make decisions quickly.

4. CONCLUSION

We present a high-speed automatic stent segmentation algorithm, which divides the problem into a series of simple and fast computations to achieve the great performance improvement. Our algorithm performs two more segmentation: guide-wire segmentation and lumen segmentation. Each step of the entire stent segmentation algorithm addresses simple problems rather quickly and passes the intermediate results to the next step, so that one complex computation takes advantage of the staged computations. The high speed and reasonable accuracy of the algorithm make it acceptable for clinicians to use in hospital operating rooms to make decisions as to whether additional treatments after a procedure is necessary or not. We are actively working on improving the precision, accuracy, and more user-friendly visualization of the segmentation results.

ACKNOWLEDGMENTS

This work is supported in part by the Engineering Research Center of Excellence Program of Korea Ministry of Education, Science and Technology(MEST) / National Research Foundation of Korea(NRF) (Grants 2012-0000469, 2012-0005256, 2012-0005633), Microsoft Research Asia, and S-Core.

REFERENCES

[1] D. Huang, E. A. Swanson, C. P. Lin, et al., "Optical coherence tomography," Science 254, 1178–1181 (1991).
[2] M. E. Brezinski, G. J. Tearney, B. E. Bouma, et al., "Imaging of coronary artery microstructure (in vitro) with optical coherence tomography," Am. J. Cardiol. 77, 92–93 (1996).
[3] G. J. Tearney, M. E. Brezinski, S. A. Boppart, et al., "Images in cardiovascular medicine. Catheter-based optical imaging of a human coronary artery," Circulation 94, 3013 (1996).

[4] J. Tanigawa, P. Barlis, C. Di Mario, “Intravascular optical coherence tomography: optimization of image acquisition and quantitative assessment of stent strut apposition,” EuroIntervention 3, 128–136 (2007).

[5] B. E. Bouma, G. J. Tearney, H. Yabushita, et al., “Evaluation of intracoronary stenting by intravascular optical coherence tomography,” Heart 89, 317–320 (2003).

[6] O. C. Raffel, J. C. Hannan, I. K. Jang, “Coronary stent malapposition as a result of a post-stenotic aneurysm detected by optical coherence tomography,” J. Invasive Cardiol. 18, 561–562 (2006).

[7] S. Tsantis, G. C. Kagadis, K. Katsanos, D. Karnabatidis, G. Bourantas, and G. C. Nikiforidis, “Automatic vessel lumen segmentation and stent strut detection in intravascular optical coherence tomography,” Medical Physics 39, 503 (2012).

[8] Z. Wang, M. W. Jenkins, H. Bezerra, M. Costa, D. Wilson, and A. Rollins, “Single-shot Stent Segmentation in Intravascular OCT Pullbacks,” Biomedical Optics (2012).

[9] N. Bruining, K. Sihan, J. Ligthart, S. de Winter, and E. Regar, “Automated three-dimensional detection of intracoronary stent struts in optical coherence tomography images,” Computing in Cardiology, 221–224 (2011).

[10] N. Otsu, “A Threshold Selection Method from Gray-Level Histograms,” Systems, Man and Cybernetics, IEEE Transactions on 9(1), 62–66 (1979).

[11] Z. Wang, H. Kyono, H. G. Bezerra, H. Wang, M. Gargesha, C. Alraies, C. Xu, J. M. Schmitt, D. L. Wilson, M. A. Costa, and A. M. Rollins, “Semiautomatic segmentation and quantification of calcified plaques in intracoronary optical coherence tomography images,” J. Biomed. Opt. 15(6), 1711 (2010).

[12] G. J. Ughi, T. Adriaenssens, K. Onsea, P. Kayaert, C. Dubois, P. Sinnaeve, M. Coosemans, W. Desmet, and J. D’hooge, “Automatic segmentation of in-vivo intra-coronary optical coherence tomography images to assess stent strut apposition and coverage,” Int. J. Cardiovasc Imaging 28(2), 229–241 (2012).

[13] G. Unal, S. Gurmeric, and S. G. Carlier, “Stent implant follow-up in intravascular optical coherence tomography images,” Int. J. Cardiovasc Imaging 26(7), 809-816 (2010).

[14] A. Wang, J. Eggermont, N. Dekker, H. M. García-García, R. Pawar, J. H. C. Reiber, and J. Dijkstra, “Automatic stent strut detection in intravascular optical coherence tomographic pullback runs,” Int. J. Cardiovasc Imaging (2012).

[15] G. T. Bonnema, K. O. Cardinal, S. K. Williams, and J. K. Barton, “An automatic algorithm for detecting stent endothelialization from volumetric optical coherence tomography datasets,” Phys. Med. Biol. 53(12), 3083–3098 (2008).